



## Original article

# Synthesis, crystal structure, DNA interaction and antioxidant activities of two novel water-soluble Cu(2+) complexes derivated from 2-oxo-quinoline-3-carbaldehyde Schiff-bases

Zeng-Chen Liu, Bao-Dui Wang, Zheng-Yin Yang\*, Yong Li, Dong-Dong Qin, Tian-Rong Li

College of Chemistry and Chemical Engineering, State Key Laboratory of Applied Organic Chemistry, Lanzhou University, Lanzhou 730000, PR China

## ARTICLE INFO

## Article history:

Received 3 March 2009

Received in revised form

4 June 2009

Accepted 5 June 2009

Available online 17 June 2009

## Keywords:

2-Oxo-quinoline-3-carbaldehyde

Schiff-bases

Crystal structure

DNA binding

Antioxidant activity

## ABSTRACT

Two novel 2-oxo-quinoline-3-carbaldehyde (4'-hydroxybenzoyl) hydrazone, thiosemicarbazone ligands and its corresponding Cu(2+) complexes were synthesized, and the two complexes' structures were determined by X-ray single crystal diffraction. The interaction of the two Cu(2+) complexes with calf thymus DNA (CT-DNA) was investigated by electronic absorption spectroscopy, fluorescence spectroscopy and viscosity measurement. The experimental evidences indicated that the two water-soluble Cu(2+) complexes could strongly bind to CT-DNA via an intercalation mechanism. The intrinsic binding constants of complexes **1** and **2** with CT-DNA were  $7.31 \times 10^6$  and  $2.33 \times 10^6 \text{ M}^{-1}$ , respectively. Furthermore, the antioxidant activities (hydroxyl radical and superoxide) of the two water-soluble metal complexes were determined by hydroxyl radical and superoxide scavenging method *in vitro*.

© 2009 Elsevier Masson SAS. All rights reserved.

## 1. Introduction

Over the past decades, the metal complexes that can interact with DNA have been extensively studied as DNA footprint, novel chemotherapeutics and highly sensitive diagnostic agents [1–6]. Generally, the transition metals play a very important role in organism and their complexes can interact non-covalently with nucleic acid by intercalation, groove-binding or external electrostatic binding for cations [3,7–11]. And that many transition metal complexes have been investigated to be utilized as probes of DNA structure, agents for mediation of strand scission of duplex DNA and chemotherapeutic agents [12–14]. Most notably, some Pt(2+) complexes (cisplatin and carboplatin) have found their way into the pharmaceutical armamentarium as applied clinical antitumor drugs [15]. Additionally, The importance of reactive oxygen species and free radicals has attracted considerable attention over the past decades. Reactive oxygen species (ROS), which include free radicals, such as hydroxyl radicals (OH<sup>•</sup>) and superoxide anion radicals (O<sub>2</sub><sup>•-</sup>) are various forms of activated oxygen. And that they are exacerbating factors in cellular injury and aging process. Antioxidants can protect the human body from free radicals and ROS effects, and

retard the progress of many chronic diseases as well as lipid peroxidation. It is well known that SOD has been investigated for use in protection against oxidative injury. However, the use of SOD protein as a therapeutic is limited by its price, charge and rapid clearance [16]. Recently study suggested that many transition metal complexes also exhibited interesting antioxidant activities (OH<sup>•</sup>, O<sub>2</sub><sup>•-</sup>, etc.) [17,18]. Therefore, it is significant to search for transition metal complexes as potential antioxidants.

Nitrogen heterocyclic compounds have been used widely in the pharmaceutical industry because of their perfect biological activities [19–23]. 2-Oxo-quinoline is a kind of alkaloid which exists in nature extensively as same as quinoline. Moreover, some derivatives of 2-oxo-quinoline have been also synthesized and investigated, because they exhibit some preferable biological activities such as antioxidation, antiproliferation, anti-inflammation and anticancer [24–27]. Also, some Schiff-bases and their metal complexes often exhibit diverse biological and pharmaceutical activities [28–32]. However, the studies on the antioxidant activities and DNA-binding mechanism of Schiff-base transition metal complexes derivated from 2-oxo-quinoline-3-carbaldehyde have not been explored. In addition, although many Schiff-base complexes exhibit good biological activities, the water-solubility of the compounds is still unsatisfactory, which restricts their actual application. In this paper, two water-soluble Cu(2+) complexes with two Schiff-base ligands are synthesized and characterized by X-ray single crystal diffraction.

\* Corresponding author. Tel.: +86 9318913515; fax: +86 9318912582.

E-mail address: [yangzy@lzu.edu.cn](mailto:yangzy@lzu.edu.cn) (Z.-Y. Yang).

The DNA-binding modes of the two Cu(2+) complexes with CT-DNA are investigated by UV-vis, fluorescence and viscosity measurements. The results show that the two water-soluble Cu(2+) complexes can interact with DNA through intercalation and the DNA-binding ability of complex **1** is higher than that of complex **2**. In addition, the two water-soluble complexes are found to possess potentially excellent antioxidant activities.

## 2. Results and discussion

The two water-soluble Cu(2+) complexes were prepared by direct reaction of ligand with appropriate mole ratios of Cu(2+) nitrate in methanol. The two complexes were air stable and soluble in water, ethanol, methanol, DMF and DMSO. The single crystal X-ray analyses showed that formula of the two Cu(2+) complexes were  $[\text{Cu}(\text{H}_2\text{L}^1)(\text{CH}_3\text{OH})]\cdot\text{NO}_3\cdot\text{CH}_3\text{OH}$  (complex **1**) and  $\text{Cu}(\text{H}_2\text{L}^2)\text{NO}_3$  (complex **2**).

Table 1 summarizes the crystal data, data collection and refinement parameters for complexes **1** and **2**.

### 2.1. Crystal structure of complexes **1** and **2**

The ORTEP representation of the structure of complex **1**, including atom numbering scheme, is shown in Fig. 1 and the selected bond lengths and bond angles are listed in Table 2. The coordination of the hydrazone with Cu(2+) results in the formation of a five-membered (CuONNC) and a six-membered (CuNCCCO) chelating rings, otherwise, there is a methanol molecule which takes part in coordination and also a non-coordinative methanol molecule, on the contrary, the  $\text{NO}_3^-$  does not coordinate with Cu(2+), and the coordination of Cu(2+) with  $\text{N}^2\text{O}^2\text{O}^4\text{O}^5$  gives a distorted quadrangular configuration. The perfect planar of  $\text{N}^3\text{C}^{10}\text{C}^{11}\text{H}$  is a consequence of  $\text{sp}^2$  hybridization rather than  $\text{sp}^3$  hybridization. In addition, the asymmetric unit cell of the complex consists of four crystallographically independent molecules of the complex.

The ORTEP representation of the structure of complex **2**, including atom numbering scheme, is shown in Fig. 2 and the selected bond lengths and bond angles are listed in Table 3. As can be seen from Fig. 2, the coordination geometry of  $\text{H}_2\text{L}^2$  with Cu(2+) is quadrangular, which is composed of a five-membered (CuNNCS)

**Table 1**  
Crystal data and structure refinement of complexes **1** and **2**.

	Complex <b>1</b>	Complex <b>2</b>
Empirical formula	$\text{C}_{11}\text{H}_9\text{CuN}_5\text{O}_4\text{S}$	$\text{C}_{19}\text{H}_{20}\text{CuN}_4\text{O}_8$
FW	370.83	495.93
Crystal color	Black	Green
Crystal size	$0.24 \times 0.27 \times 0.32$ mm	$0.35 \times 0.31 \times 0.22$ mm
Crystal system	Triclinic	Monoclinic
Space group	<i>p</i> -1	<i>p</i> 21 <i>c</i>
<i>a</i> (Å)	8.3415(9)	7.7826(4)
<i>b</i> (Å)	8.7979(9)	27.6765(14)
<i>c</i> (Å)	10.6365(11)	9.6798(5)
$\alpha$	94.747(2)	90
$\beta$	111.701(2)	102.548(2)
$\gamma$	110.179(2)	90
Volume (Å <sup>3</sup> )	660.66(12)	2035.18(18)
<i>Z</i>	2	4
<i>D</i> <sub>calc</sub> (Mg m <sup>-3</sup> )	1.864	1.619
Abs coeff. (mm <sup>-1</sup> )	1.838	1.130
<i>F</i> (000)	374	1020
$\theta_{\text{min}}$ and $\text{max}$ (deg)	2.12–26	1.47–27
Reflections collected/ unique	3626/2560 [R(int) = 0.0122]	12365/4397 [R(int) = 0.0313]
Final <i>R</i> indices [ <i>I</i> > 2σ( <i>I</i> )]	<i>R</i> <sub>1</sub> = 0.0311, <i>wR</i> <sub>2</sub> = 0.0938	<i>R</i> <sub>1</sub> = 0.0364, <i>wR</i> <sub>2</sub> = 0.0951
<i>R</i> indices (all data)	<i>R</i> <sub>1</sub> = 0.0349, <i>wR</i> <sub>2</sub> = 0.0965	<i>R</i> <sub>1</sub> = 0.0517, <i>wR</i> <sub>2</sub> = 0.1030

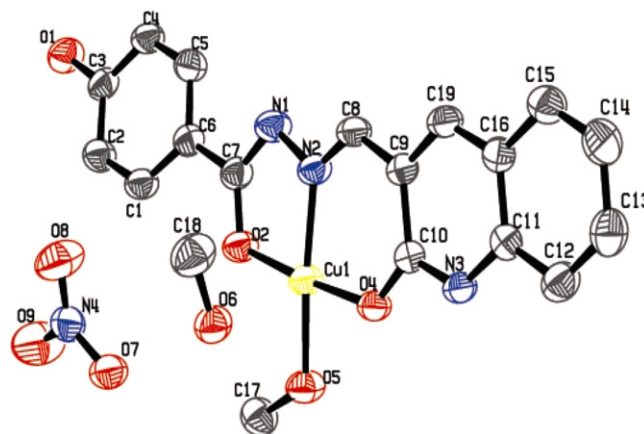


**Fig. 1.** ORTEP view of  $[\text{CuL}^1]$  showing the atom numbering of scheme and 50% thermal ellipsoids probability for the non-hydrogen atoms.

and a six-membered (CuNCCCO) chelating rings and a nitrate which is a monodentate, and the planar quadrangle may be a little distorted as a result of the hydrogen bond between the  $\text{O}^3$  and hydrogen atoms of other molecules. In addition, the  $\text{C}=\text{S}$  bond (1.743 Å) has been found to be enolic and  $\text{N}^1\text{C}^9\text{H}$  gives a perfect planar configuration as a consequence of  $\text{sp}^2$  hybridization. In addition, the asymmetric unit cell of the complex consists of four crystallographically independent molecules of the complex.

### 2.2. DNA-binding studies

#### 2.2.1. Electronic absorption titration

Electronic absorption spectroscopy is one of the most useful techniques for studying binding mode of metal complexes to DNA

**Table 2**  
Selected bond lengths (Å) and angles (°) for complex **1**.

Bond names	Bond lengths (Å)	Bond angles	Angle (°)
Cu(1)–O(2)	1.9123(15)	O(2)–Cu(1)–O(4)	174.76(6)
Cu(1)–O(4)	1.9204(15)	O(2)–Cu(1)–N(2)	81.71(7)
Cu(1)–N(2)	1.9235(19)	O(4)–Cu(1)–N(2)	93.32(7)
Cu(1)–O(5)	1.9557(18)	O(2)–Cu(1)–O(5)	94.73(8)
C(7)–O(2)	1.295(3)	O(4)–Cu(1)–O(5)	90.45(7)
C(7)–N(1)	1.320(3)	N(2)–Cu(1)–O(5)	169.12(9)
C(8)–N(2)	1.291(3)	C(1)–C(6)–C(5)	118.0(2)
C(8)–C(9)	1.436(3)	C(1)–C(6)–C(7)	120.0(2)
C(8)–H(8)	0.9300	C(5)–C(6)–C(7)	122.0(2)
C(9)–C(19)	1.368(3)	O(2)–C(7)–N(1)	124.2(2)
C(9)–C(10)	1.452(3)	O(2)–C(7)–C(6)	117.8(2)
C(10)–O(4)	1.270(3)	N(1)–C(7)–C(6)	117.9(2)
C(10)–N(3)	1.341(3)	N(2)–C(8)–C(9)	124.2(2)
C(11)–C(12)	1.390(3)	N(2)–C(8)–H(8)	117.9
C(11)–C(16)	1.399(3)	C(9)–C(8)–H(8)	117.9
N(2)–N(1)	1.384(3)	O(4)–C(10)–N(3)	117.54(19)
N(3)–H(3N)	0.78(3)	N(3)–C(10)–C(9)	116.59(19)
O(7)–C(3)	1.215(3)	C(7)–N(1)–N(2)	108.89(19)
N(4)–O(9)	1.226(3)	C(8)–N(2)–N(1)	117.71(19)
N(4)–O(7)	1.253(3)	C(8)–N(2)–Cu(1)	127.69(16)
C(17)–O(5)	1.428(3)	N(1)–N(2)–Cu(1)	114.57(15)
C(18)–O(6)	1.395(3)	C(10)–N(3)–C(11)	125.7(2)
O(1)–H(1A)	0.8200	C(10)–N(3)–H(3N)	114.6(18)
O(5)–H(5O)	0.66(3)	C(11)–N(3)–H(3N)	119.6(18)
O(6)–H(6)	0.8200	C(3)–O(1)–H(1A)	109.5
C(11)–N(3)	1.379(3)	C(7)–O(2)–Cu(1)	110.54(13)
		C(10)–O(4)–Cu(1)	126.85(14)
		C(17)–O(5)–Cu(1)	125.42(16)
		C(17)–O(5)–H(5O)	119(3)
		Cu(1)–O(5)–H(5O)	106(3)
		C(18)–O(6)–H(6)	109.5
		O(4)–C(10)–C(9)	125.87(19)

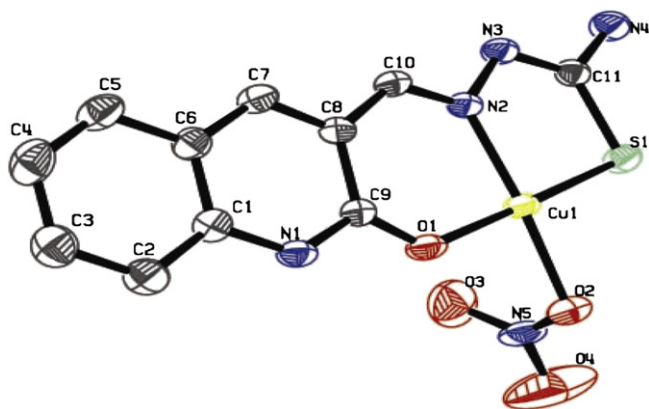


**Fig. 2.** ORTEP view of  $[\text{CuL}_2]$  showing the atom numbering of scheme and 50% thermal ellipsoids probability for the non-hydrogen atoms.

[33,34]. The UV–vis absorption spectra of complexes **1** and **2** in the absence or presence of CT-DNA are shown in Fig. 3. The absorption bands of complex **1** at 206 and 260 nm exhibit hypochromism of about 30.76% and 72.00%, respectively. Moreover, complex **2** at 206 and 260 nm exhibit hypochromism of about 30.56% and 37.50%, respectively. These results suggest that the complex **1** show stronger hypochromicity than complex **2**. Furthermore, it also likely intimates that the two water-soluble  $\text{Cu}(2+)$  complexes can bind to the helix via intercalation in the Tris–HCl (pH = 7.2) which do not contain any organic solvent. After the complexes intercalate to the base pair of DNA, the  $\pi^*$  orbital of the intercalated ligand on the complexes can couple with  $\pi$  orbital of the base pairs, thus decreasing the  $\pi$ – $\pi^*$  transition energies. On the other hand, the

**Table 3**

Selected bond lengths (Å) and angles ( $^\circ$ ) for complex **2**.

Bond names	Bond lengths (Å)	Bond angles	Angle ( $^\circ$ )
Cu(1)–O(1)	1.9360(18)	O(1)–Cu(1)–N(2)	93.08(8)
Cu(1)–N(2)	1.9728(19)	O(1)–Cu(1)–O(2)	90.37(8)
Cu(1)–O(2)	2.0401(18)	N(2)–Cu(1)–O(2)	168.06(8)
Cu(1)–S(1)	2.2393(7)	O(1)–Cu(1)–S(1)	177.76(6)
C(1)–N(1)	1.373(3)	N(2)–Cu(1)–S(1)	85.71(6)
C(1)–C(2)	1.392(3)	O(2)–Cu(1)–S(1)	90.45(6)
C(1)–C(6)	1.404(3)	C(9)–N(1)–C(1)	126.5(2)
C(2)–C(3)	1.377(4)	C(9)–N(1)–H(1N)	118(3)
C(2)–H(2)	0.9300	C(1)–N(1)–H(1N)	115(3)
C(3)–C(4)	1.403(4)	C(10)–N(2)–N(3)	114.3(2)
C(3)–H(3)	0.9300	C(10)–N(2)–Cu(1)	125.04(16)
C(4)–C(5)	1.357(4)	N(3)–N(2)–Cu(1)	120.66(15)
C(4)–H(4)	0.9300	C(11)–N(3)–N(2)	113.1(2)
C(5)–C(6)	1.415(4)	C(11)–N(4)–H(3N)	117(2)
C(5)–H(5)	0.9300	C(11)–N(4)–H(4N)	117(3)
C(6)–C(7)	1.411(4)	H(3N)–N(4)–H(4N)	125(4)
C(7)–C(8)	1.365(4)	O(2)–N(5)–O(3)	122.3(3)
C(7)–H(7)	0.9300	O(2)–N(5)–O(4)	118.3(3)
C(8)–C(10)	1.441(3)	O(3)–N(5)–O(4)	119.3(3)
C(8)–C(9)	1.453(3)	C(9)–O(1)–Cu(1)	127.76(16)
C(9)–O(1)	1.246(3)	N(5)–O(2)–Cu(1)	107.74(16)
C(9)–N(1)	1.348(3)	C(11)–S(1)–Cu(1)	95.04(9)
C(10)–N(2)	1.287(3)		
C(10)–H(10)	0.9300		
C(11)–N(3)	1.311(3)		
C(11)–N(4)	1.340(3)		
C(11)–S(1)	1.743(2)		
N(1)–H(1N)	0.69(3)		
N(2)–N(3)	1.394(3)		
N(4)–H(3N)	0.86(4)		
N(4)–H(4N)	0.74(4)		
N(5)–O(2)	1.215(3)		
N(5)–O(3)	1.228(3)		
N(5)–O(4)	1.249(4)		

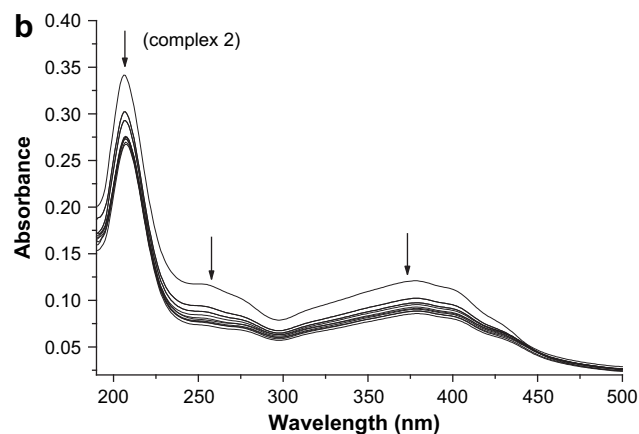
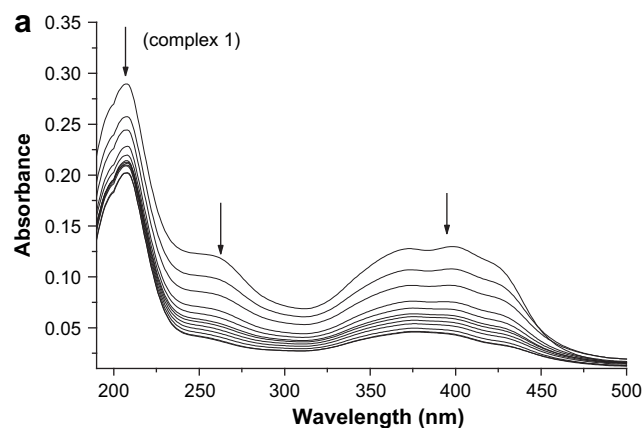


**Fig. 3.** (a) Electronic spectra of complex **1** (10  $\mu\text{M}$ ) in the presence of increasing amounts of CT-DNA (0–10  $\mu\text{M}$ ). Arrow shows the absorbance changes upon increasing DNA concentration. (b) Electronic spectra of complex **2** (10  $\mu\text{M}$ ) in the presence of increasing amounts of CT-DNA (0–10  $\mu\text{M}$ ). Arrow shows the absorbance changes upon increasing DNA concentration.

coupling  $\pi^*$  orbital are partially filled by electrons, thus decreasing the transition probabilities [35,36].

### 2.2.2. Fluorescence spectra

The two  $\text{Cu}(2+)$  complexes exhibit weak luminescence in Tris–HCl buffer with a maximum wavelength of about 400 and 450 nm. The results of the emission titration for the two complexes with helix DNA (CT-DNA) that are illustrated in the titration curves are shown in Fig. 4. Upon the addition of CT-DNA, the emission intensities at about 450 nm of the two complexes increase by around 1.41 and 1.20 times for complexes **1** and **2**, respectively. In addition, corresponding 5 and 6 nm blue shifts emerge with the increase of emission intensities. The results of emission titration suggest that the two water-soluble complexes are all protected from solvent water molecules by the hydrophobic environment inside the DNA helix; as a result, the accessibility of solvent water molecules to these compounds is reduced. Compared to the intensity enhancement of the two complexes in the presence of CT-DNA, complex **1** has preferable DNA-binding ability than complex **2**. In order to illustrate quantitatively the consequence, changes in emission intensities at about 450 nm for the two  $\text{Cu}(2+)$  complexes have been plotted against the added DNA concentration per mole of complexes. According to the Scatchard equation [37–39], a plot of  $r/C_f$  versus  $r$  gives the binding constants of complexes **1** and **2**. The results imply that both the compounds can insert between DNA base pairs and complex **1** ( $K = 7.31 \times 10^6$ ) can interact with DNA more strongly than complex **2** ( $K = 2.33 \times 10^6$ ).

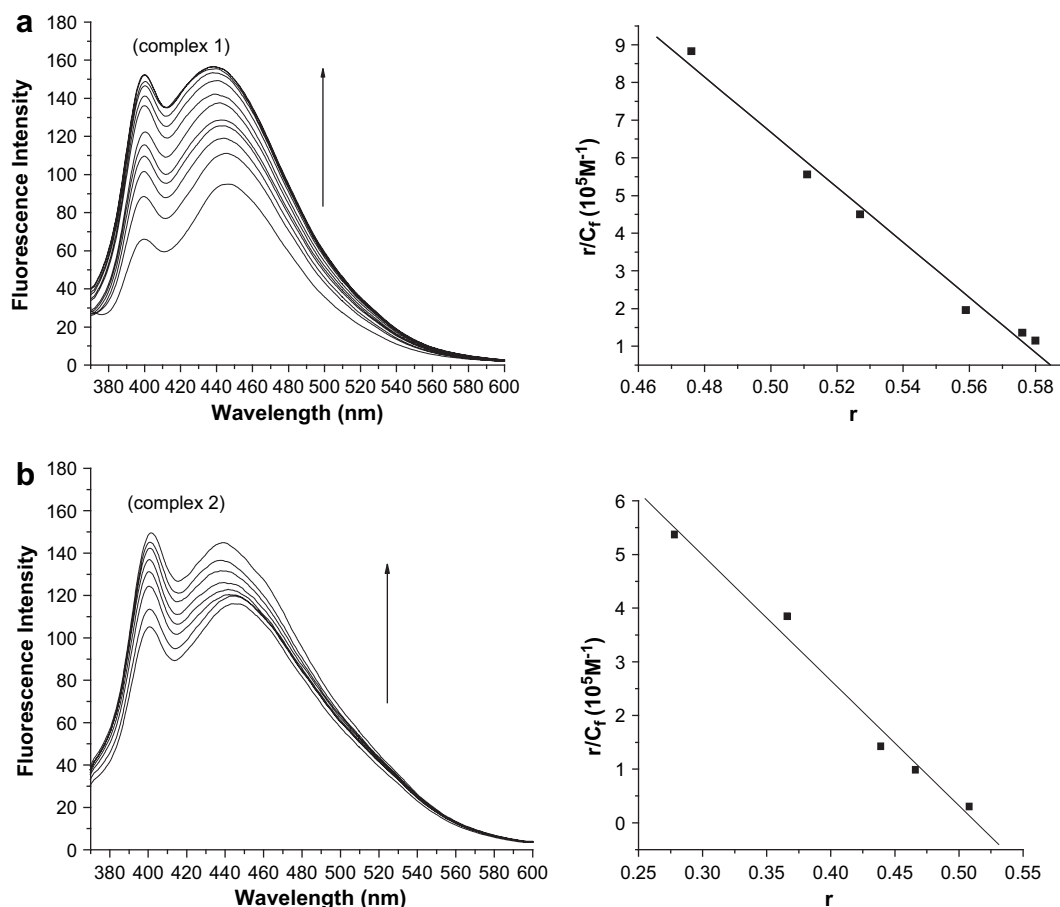


**Fig. 4.** (a) The emission enhancement spectra of complex **1** ( $10 \mu\text{M}$ ) in the presence of 0, 2.5, 5.0, 7.5, 10.0, 12.5, 15.0, 17.5 and  $20.0 \mu\text{M}$  CT-DNA. Arrow shows the emission intensity changes upon increasing DNA concentration. Inset: Scatchard plot of the fluorescence titration data of complex **1**,  $K = 7.31 \times 10^6$ . (b) The emission enhancement spectra of complex **2** ( $10 \mu\text{M}$ ) in the presence of 0, 2.5, 5.0, 7.5, 10.0, 12.5, 15.0 and  $17.5 \mu\text{M}$  CT-DNA. Arrow shows the emission intensity changes upon increasing DNA concentration. Inset: Scatchard plot of the fluorescence titration data of complex **2**,  $K = 2.33 \times 10^6$ .

### 2.2.3. EB-DNA experiment

The DNA-binding modes of compound are further monitored by fluorescent EB displacement assay. It is well known that EB can emit intense fluorescence due to strong intercalation nonspecifically between DNA base pairs [40,41]. Competitive binding of other drugs to DNA and EB will result in displacement of bound EB and decrease in the fluorescence intensity. This fluorescence-based competition technique can provide indirect evidence for the DNA-binding mode. Fig. 5 shows the emission spectra of DNA-EB spectra with increasing amounts of the two water-soluble  $\text{Cu}(2+)$  complexes. The emission intensity of the DNA-EB system ( $\lambda_{\text{em}} = 587 \text{ nm}$ ) decrease apparently with the increasing concentration of the  $\text{Cu}(2+)$  complexes. The quenching plots illustrate that the quenching of EB bound to DNA by the complexes are in good agreement with the linear Stern-Volmer equation. The fluorescence quenching is caused by EB changing from a hydrophobic environment into an aqueous environment. And the fluorescence quenching phenomenon at  $587 \text{ nm}$  of the DNA-EB system indicates that the two water-soluble  $\text{Cu}(2+)$  complexes can displace EB from the DNA-EB system. Such a characteristic change is often observed in intercalative DNA interaction.

### 2.2.4. Viscosity measurement

As a mean for further clarifying the binding mode of complex to DNA, the viscosity measurements are also carried out [42,43]. Fig. 6 shows the relative viscosity change of DNA in the presence of

varying amounts of the two water-soluble complexes **1** and **2**. The results indicate that the viscosity of DNA increase on addition of the concentrations of complexes **1** and **2**. As general viewpoint, the viscosities of DNA increase steadily when the compounds intercalate between adjacent DNA base pairs. This illustrate that the two water-soluble  $\text{Cu}(2+)$  complexes can interact with DNA through an intercalative mode and complex **1** can bind to CT-DNA more tightly than complex **2**. In addition, the results obtained from viscosity are consistent with that obtained from the spectroscopic studies.

### 2.3. Antioxidant activity

Fig. 7a depicts the inhibitory effect of the complexes on  $\text{OH}^\cdot$ . The inhibitory of the complexes is marked and suppression ratio increases with increasing complexes concentration in the range of tested concentration. The sequence of the suppression ratio for  $\text{OH}^\cdot$  is complex **1** > complex **2** at different concentration. Moreover, mannitol and Vitamin C are well-known natural antioxidant compounds, so we compare the two water-soluble  $\text{Cu}(2+)$  complexes with them in the same way. As reported in previous paper [36]. The 50% inhibitory concentration ( $\text{IC}_{50}$ ) value of mannitol is about  $9.6 \text{ mM}$ . The antioxidant experiments testify that complex **1** ( $\text{IC}_{50} = 4 \mu\text{M}$ ) and complex **2** ( $\text{IC}_{50} = 5 \mu\text{M}$ ) represent very excellent antioxidant ( $\text{OH}^\cdot$ ) activities which are much better than that of standard antioxidants like mannitol and Vitamin C [44].

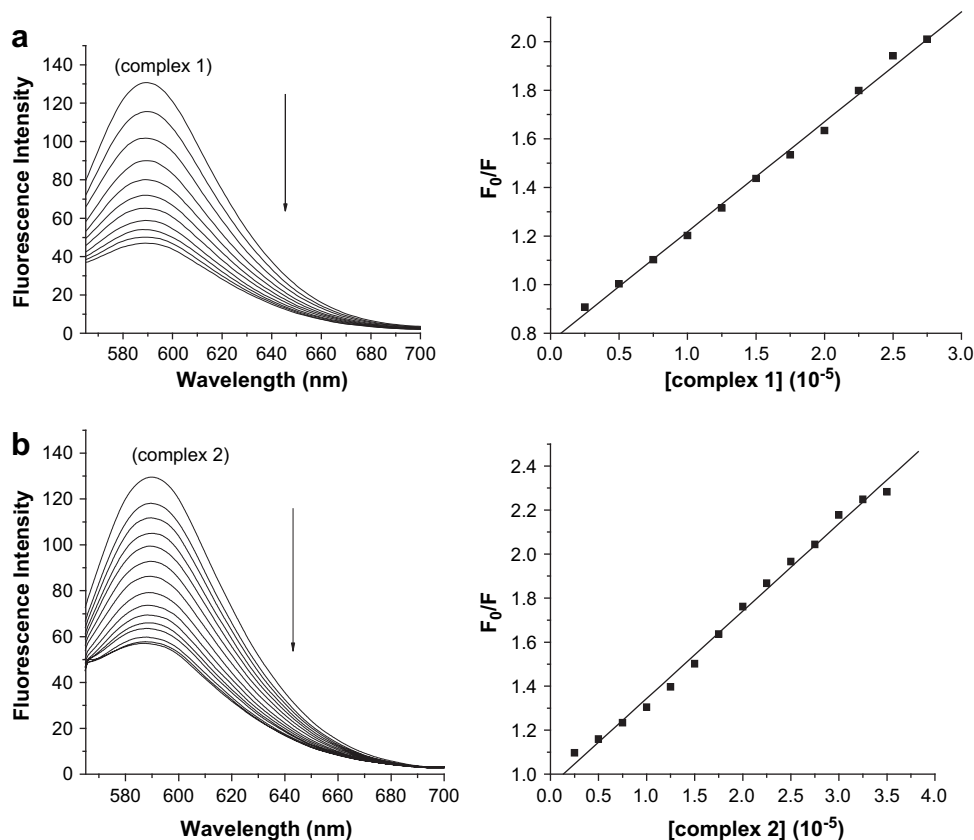


**Fig. 5.** (a) The emission spectra of DNA-EB system,  $\lambda_{em} = 587$  nm, in the presence of 0, 5, 10, 15, 20, 25, 30, 35, 40 and 45  $\mu\text{M}$  complex **1**. Arrow shows the emission intensity changes upon increasing complex concentration. Inset: Stern-Volmer plot of the fluorescence titration data of complex **1**,  $K_q = 5.91 \times 10^4$ . (b) The emission spectra of DNA-EB system,  $\lambda_{em} = 587$  nm, in the presence of 0, 5, 10, 15, 20, 25, 30, 35, 40, 45, 50, 55 and 60  $\mu\text{M}$  complex **2**. Arrow shows the emission intensity changes upon increasing complex concentration. Inset: Stern-Volmer plot of the fluorescence titration data of complex **2**,  $K_q = 3.97 \times 10^4$ .

Fig. 7b shows that the inhibitory of two complexes on superoxide radical is also related to concentration, at the range from 1.0 to 5.0  $\mu\text{M}$ , the percentage scavenging effect valued from 48.56% to 82.34% for complex **1** and from 38.20% to 72.56% for complex **2**. It illuminates that the two water-soluble  $\text{Cu}(2+)$  complexes exhibit

perfect ability to suppress  $\text{O}_2^{\cdot-}$ , and the suppression ratio of complex **1** ( $\text{IC}_{50} = 1.0 \mu\text{M}$ ) is higher than that of complex **2** ( $\text{IC}_{50} = 3.5 \mu\text{M}$ ).

### 3. Conclusions

In summary, two new water-soluble  $\text{Cu}(2+)$  complexes of 2-oxo-quinoline-3-carbaldehyde (4'-hydroxybenzoyl) hydrazone and thiosemicarbazone were evidenced to interact with DNA by intercalation and could be potential anticancer reagents. And that compared with the  $\text{Cu}(2+)$  complex of 2-oxo-quinoline-3-carbaldehyde thiosemicarbazone, complex **1** demonstrated that there was preferable DNA-binding property as a result of the strong stacking interaction between an aromatic chromophore and the base pairs of DNA. Simultaneously, the water-solution activities of the two complexes could enhance the biological compatibility *in vivo*. In addition, the two water-soluble  $\text{Cu}(2+)$  complexes of Schiff-bases also exhibited excellent antioxidant (hydroxyl radical  $\text{OH}^{\cdot}$  and superoxide radical  $\text{O}_2^{\cdot-}$ ) activities and the antioxidant activity of complex **1** is better than that of complex **2** due to the existence of hydroxyl of 2-oxo-quinoline-3-carbaldehyde (4'-hydroxybenzoyl) hydrazone [45].

### 4. Experimental

#### 4.1. Instrumentation

$^1\text{H}$  NMR spectra were recorded on a Varian VR300-MHz spectrometer with TMS as an internal standard. The melting points of

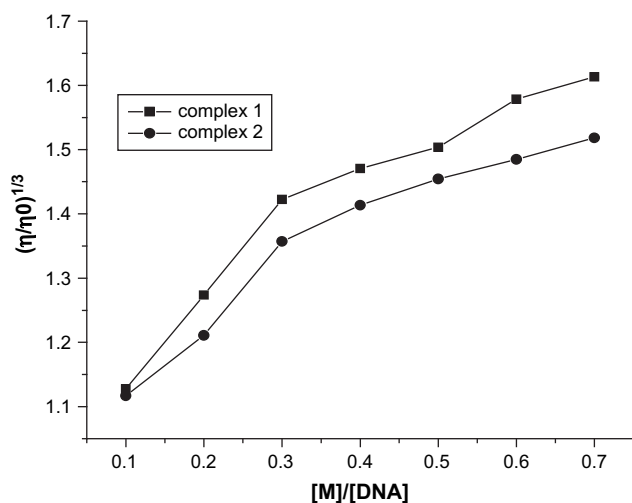


**Fig. 6.** Effect of increasing amounts of complex **1** (■) and complex **2** (●) on the relative viscosity of calf thymus DNA at  $25(\pm 0.1)^\circ\text{C}$ .

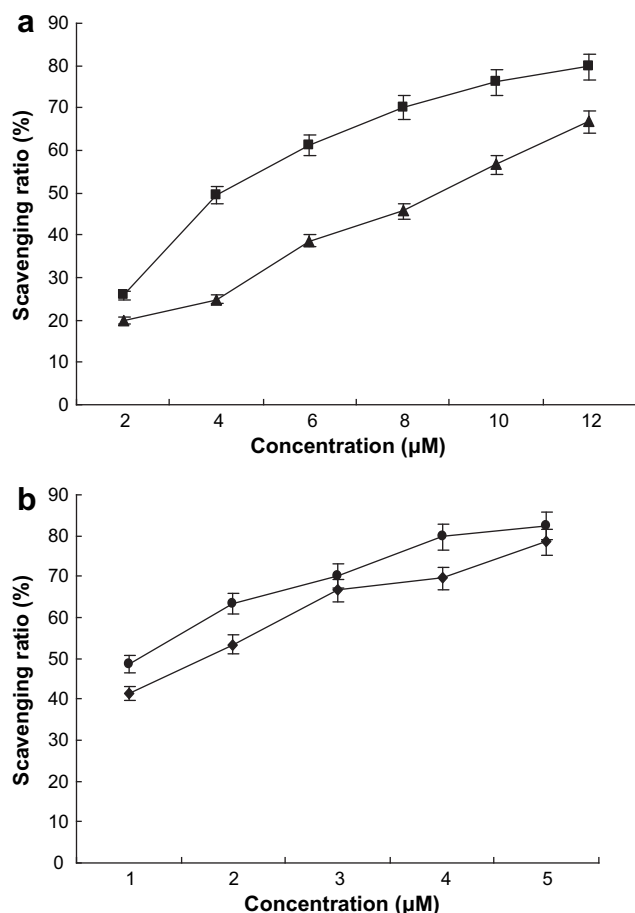


**Fig. 7.** (a) Scavenging effect of Cu(2+) complexes on hydroxyl radicals. (■) complex **1**; (▲) complex **2**. Experiments were performed in triplicate. Values are expressed as mean  $\pm$  standard deviation ( $n = 1$ ). (b) Scavenging ratio of the two Cu(2+) complexes on superoxide. (●) complex **1**; (◆) complex **2**. Experiments were performed in triplicate. Values are expressed as mean  $\pm$  standard deviation ( $n = 1$ ).

the compound were determined on a Beijing XT4-100X microscopic melting point apparatus. The UV-vis spectra were recorded on a Perkin-Elmer Lambda-35 UV-vis spectrophotometer. Fluorescence spectra were obtained on a Shimadzu RF-5301 spectrophotometer at room temperature. The antioxidant activities were performed in water with 721E spectrophotometer (Shanghai Analytical Instrument factory China).

#### 4.2. Materials

CT-DNA, ethidium bromide (EB), nitro-bluetetrazolium (NBT), methionine (MET) and Vitamin B<sub>2</sub> (VitB<sub>2</sub>) were purchased from Sigma Chemical Co. Acetanilide was purchased from Guang Fu Chemical Co., Tianjin, China. All materials and solvents were of analytical reagent grade quality and were used without further purification.  $M(\text{NO}_3)_2 \cdot n\text{H}_2\text{O}$  ( $M = \text{Cu}$ ) were from China. Tris-HCl buffer,  $\text{KH}_2\text{PO}_4$ - $\text{Na}_2\text{HPO}_4$  buffers and EDTA-Fe(2+) were prepared with twice distilled water.

All the experiments involving the interaction of the two water-soluble complexes with CT-DNA were carried out in doubly distilled water containing 5 mM Tris [Tris(hydroxymethyl)-aminomethane] and 50 mM NaCl and adjusted to pH = 7.2 with hydrochloric acid. Solution of CT-DNA gave ratios of absorbance at 260 and 280 nm of about 1.8–1.9:1, indicating that the CT-DNA was sufficiently free of protein. The CT-DNA concentration per nucleotide was determined

spectrophotometrically by employing an extinction coefficient of  $6600 \text{ M}^{-1} \text{ cm}^{-1}$  at 260 nm.

#### 4.3. Synthesis of ligands $\text{H}_2\text{L}^1$ and $\text{H}_2\text{L}^2$

As shown in Scheme 1 2-oxo-quinoline-3-carbaldehyde was prepared according to the literature [46]. An ethanol solution containing 4-hydroxybenzoyl hydrazine was added to another ethanol solution containing 2-oxo-quinoline-3-carbaldehyde. The mixture was refluxed for 12 h with stirring and a yellow precipitate was separated out. The precipitation was filtrated under decompression and washed with ethanol. Recrystallization from DMF/ $\text{H}_2\text{O}$  (V:V = 1:1) gave the ligand  $\text{H}_2\text{L}^1$ , which was dried under vacuum. Yield 85%; m.p. 298–300 °C.  $^1\text{H NMR}$  (DMSO- $d_6$ , ppm):  $\delta$  12.066 (1H, s, -OH), 12.023 (1H, s, -N<sup>1</sup>H-), 11.866 (1H, s, -N<sup>3</sup>H-), 8.715 (1H, s, -CH=N-), 8.496 (1H, s, 19-H), 7.863–7.922 (2H, s, 1,5-H), 7.527–7.578 (1H, m, 12-H), 7.424–7.475 (1H, m, 13-H), 7.322–7.359 (1H, m, 15-H), 7.201–7.250 (1H, m, 14-H), 6.931–6.990 (2H, m, 2,4-H).

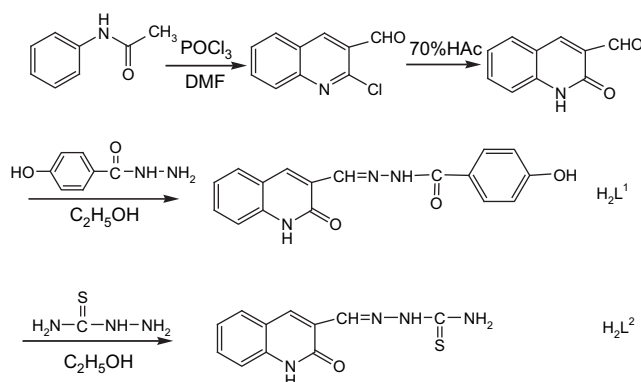
The ligand  $\text{H}_2\text{L}^2$  was synthesized according to the same procedure as the synthesis method of ligand  $\text{H}_2\text{L}^1$ . Yield 76%; m.p. 314–316 °C.  $^1\text{H NMR}$  (DMSO- $d_6$ , ppm):  $\delta$  12.003 (1H, s, -N<sup>3</sup>H-), 11.643 (1H, s, -N<sup>1</sup>H-), 8.769 (1H, s, 7-H), 8.286–8.310 (2H, m, -NH<sub>2</sub>), 8.103 (1H, s, 7-H), 7.636–7.661 (1H, m, 2-H), 7.497–7.554 (1H, m, 3-H), 7.310–7.337 (1H, m, 5-H), 7.196–7.249 (1H, m, 4-H).

#### 4.4. Preparation of Cu(2+) complexes

The ligand  $\text{H}_2\text{L}^1$  (0.2 mmol, 0.0492 g) and the Cu(2+) nitrate (0.2 mmol, 0.0483 g) were added to methanol. After 5 min, the mixtures were filtered to remove any insoluble residues and then were stirred for 10 h under reflux. A pitchy precipitate (complex **1**) was separated from the solution by suction filtration, purified by washing several times with ethanol and dried for 24 h under vacuum. Complex **2** was prepared by the same method. Complexes **1** and **2** were pitchy and green powers, respectively. But the crystal of complex **1** was black.

#### 4.5. X-ray crystallography

The single crystals of two water-soluble complexes were gained in the methanol using diffusing method. A black crystal of complex **1** ( $0.24 \times 0.27 \times 0.32$  mm) was measured on a Bruker Smart-1000 CCD diffractometer with graphite monochromatic Mo K $\alpha$  radiation ( $\lambda = 0.71073 \text{ \AA}$ ) at 296(2) K,  $2.12^\circ < \theta < 26^\circ$  for  $hkl$  ( $-10 \leq h \leq 9$ ,  $-10 \leq k \leq 10$ ,  $-10 \leq l \leq 13$ ) in the triclinic. A green crystal of complex **2** ( $0.35 \times 0.31 \times 0.22$  mm) was measured on a Bruker



**Scheme 1.** Preparation of the ligands.

Smart-1000 CCD diffractometer with graphite monochromatic Mo K $\alpha$  radiation ( $\lambda = 0.71073 \text{ \AA}$ ) at 296(2) K,  $1.47^\circ < \theta < 27^\circ$  for  $hkl$  ( $-9 \leq h \leq 9$ ,  $-35 \leq k \leq 33$ ,  $-12 \leq l \leq 11$ ) in the monoclinic. The positions and anisotropic thermal parameters of all non-hydrogen atoms were refined on  $F^2$  by full-matrix least-squares techniques with the SHELX-97 program package [47]. Absorption correction was employed using Semi-empirical methods from equivalents.

#### 4.6. DNA-binding study methods

##### 4.6.1. Electronic absorption spectroscopy

The Cu(2+) complexes were dissolved in Tris–HCl buffer (5 mM Tris–HCl; 50 mM NaCl, pH = 7.2). The example of fixed amount compounds (10  $\mu\text{M}$ ) were titrated with increasing amounts of DNA, over a range of DNA concentrations from 0 to 10  $\mu\text{M}$ .

##### 4.6.2. Fluorescence spectroscopy

In order to affirm quantitatively the affinity of the two water-soluble complexes binding to DNA, the intrinsic binding constant  $K$  of the Cu(2+) complexes was obtained by the electronic absorption spectroscopy method. The two water-soluble complexes were dissolved in Tris–HCl buffer (5 mM Tris–HCl; 50 mM NaCl, pH = 7.2) at concentration 10  $\mu\text{M}$ . The fluorescence titration experiments were performed with fixed concentration of drugs (10  $\mu\text{M}$ ) while gradually increasing the concentration of CT-DNA with the range from 2.5 to 25  $\mu\text{M}$ .  $K$  values were determined using the following equation.

$$r/C_f = K_b(1 - nr)$$

where  $r = C_b/[DNA]$ ,  $C_f = C_t [(F - F^0)/(F^{\text{max}} - F^0)]$ ,  $C_b$  and  $C_t$  is the concentration of free compound and the total compound, respectively.  $F$  is the observed fluorescence emission intensity at a given DNA concentration,  $F^0$  is the intensity in the absence of DNA, and  $F^{\text{max}}$  is the fluorescence intensity of the totally bound compound. Binding data were casted into the form of a Scatchard plot of  $r/C_f$  versus  $r$ . All experiments were conducted at 20 °C in a buffer containing 5 mM Tris–HCl (pH = 7.2) and 50 mM NaCl.

##### 4.6.3. EB displacement experiment

Further support for the two water-soluble Cu(2+) complexes binding to DNA via intercalation was given through the emission quenching experiment. A 2 mL solution of 5  $\mu\text{M}$  DNA and 0.4  $\mu\text{M}$  EB was titrated by complexes ( $\lambda_{\text{ex}} = 525 \text{ nm}$ ,  $\lambda_{\text{em}} = 587 \text{ nm}$ , slit = 10 nm). According to the classical Stern–Volmer equation

$$F_0/F = K_q[Q] + 1$$

where  $F_0$  is the emission intensity in the absence of quencher,  $F$  is the emission intensity in the presence of quencher,  $K_q$  is the quenching constant, and  $[Q]$  is the quencher concentration. The plots can be used to characterize the quenching as being predominantly dynamic or static. Plots of  $F_0/F$  versus  $[Q]$  appear to be linear.

##### 4.6.4. Viscosity measurements

Hydrodynamic method, such as determination of viscosity, which is exquisitely sensitive to the change of length of DNA, may be the most effective means of studying the binding mode of complexes with DNA. To further confirm the interaction mode of the two water-soluble Cu(2+) complexes with DNA, a viscosity study was carried out. Viscosity measurements were conducted on an Ubbelohde viscometer, immersed in a thermostated water bath maintained at 25.0( $\pm$ 0.1) °C. Data were presented as  $(\eta/\eta^0)^{1/3}$  versus the ratio of the concentration of the compound and CT-DNA, where  $\eta$  was the viscosity of CT-DNA in the presence of the compound and  $\eta^0$  was the viscosity of CT-DNA alone. Viscosity

values were calculated from the observed flow time of DNA containing solution corrected from the flow time of buffer alone ( $t_0$ )  $\eta = t - t_0$ .

#### 4.7. Scavenger measurements of hydroxyl radical (OH $\cdot$ ) and superoxide radical (O $_2^{\cdot-}$ )

The hydroxyl radical (OH $\cdot$ ) in aqueous media was generated by the Fenton system. The solution of the tested complex was prepared with two distilled water. The 5 mL assay mixture contained following reagents: safranin (11.4  $\mu\text{M}$ ), EDTA–Fe(2+) (40  $\mu\text{M}$ ), H $_2$ O $_2$  (1.76 mM), the tested complex (1–6  $\mu\text{M}$ ) and a phosphate buffer (67  $\mu\text{M}$ , pH = 7.4). The assay mixtures were incubated at 30 °C for 10 min in a water bath. After that, the absorbance was measured at 520 nm. All the tests were run in triplicate and expressed as the mean and ( $\pm$ ) standard deviation (SD).

$$\text{Scavenging ratio(\%)} = [(A_i - A_0)/(A_c - A_0)] \times 100$$

where  $A_i$  = the absorbance in the presence of the tested compound;  $A_0$  = the absorbance in the absence of the tested compound;  $A_c$  = the absorbance in the absence of the tested compound, EDTA–Fe(2+) and H $_2$ O $_2$ .

The superoxide radical (O $_2^{\cdot-}$ ) was produced by the system of MET/VitB $_2$ /NBT and determined spectrophotometrically by NBT photoreduction method with a little modification in the method adopted elsewhere [48–50]. The amount of O $_2^{\cdot-}$  could be calculated by measuring the absorbance at 560 nm. Solution of VitB $_2$  and NBT were prepared under the condition of avoiding light. The tested compounds were dissolved in water. The assay mixture, in a total volume of 5 mL, contained MET (10 mM), NBT (46  $\mu\text{M}$ ), VitB $_2$  (3.3  $\mu\text{M}$ ), the tested compound (1–6  $\mu\text{M}$ ) and a phosphate buffer (67  $\mu\text{M}$ , pH = 7.8). After illuminating with a fluorescent lamp at 30 °C for 10 min, the absorbance of the samples ( $A_i$ ) was measured at 560 nm. The sample without the tested compound was used as control and its absorbance was  $A_0$ . All experimental results were expressed as the mean and ( $\pm$ ) standard deviation (SD) of triplicate determinations. The suppression ratio for O $_2^{\cdot-}$  was calculated from the following expression. The scavenging ratio  $\eta_a = (A_0 - A_i)/A_0 \times 100\%$  [51].

#### 5. Supplementary data

Crystallographic data for the structural analysis have been deposited with the Cambridge Crystallographic Data Centre, CCDC (719432, 719431). Copy of this information may be obtained free of charge from the Director, CCDC, 12 Union Road, Cambridge, CB2 1EZ, UK (fax: +44 1223 336033; e-mail: [deposit@ccdc.cam.ac.uk](mailto:deposit@ccdc.cam.ac.uk) or <http://www.ccdc.cam.ac.uk/submit>).

#### Acknowledgement

This work is supported by the National Natural Science Foundation of China (20475023) and Gansu NSF (0710RJZA012).

#### References

- [1] A.M. Pyle, J.K. Barton, *Prog. Inorg. Chem.* 38 (1990) 413–475.
- [2] T.D. Tullius. In *Metal–DNA Chemistry*. Ed. ACS Symposium Series. ACS Washington, D.C. 402 (1989) 1–23.
- [3] C. Metcalfe, J.A. Thomas, *Chem. Soc. Rev.* 32 (2003) 215–224.
- [4] K.E. Erkkila, D.T. Odom, J.K. Barton, *Chem. Rev.* 99 (1999) 2777–2796.
- [5] F. Liang, P. Wang, X. Zhou, T. Li, Z.Y. Li, H.K. Lin, D.Z. Gao, C.Y. Zheng, C.T. Wu, *Bioorg. Med. Chem. Lett.* 14 (2004) 1901–1904.
- [6] K. Jiao, Q.X. Wang, W. Sun, F.F. Jian, *J. Inorg. Biochem.* 99 (2005) 1369–1375.
- [7] S. Arturo, B. Giampaolo, R. Giuseppe, G.L. Maria, T. Salvatore, *J. Inorg. Biochem.* 98 (2004) 589–594.

- [8] H. Catherine, P. Marguerite, R. Michael, G.S. Stephanie, M. Bernard, J. Biol. Inorg. Chem. 6 (2001) 14–17.
- [9] B. Macias, M.V. Villa, E. Fiz, I. Garcia, A. Castineiras, M.G. Alvarez, J. Borrás, J. Inorg. Biochem. 88 (2002) 101–107.
- [10] H. Zhang, C.S. Liu, X.H. Bu, M. Yang, J. Inorg. Biochem. 99 (2005) 1119–1129.
- [11] S. Sharma, S.K. Singh, M. Chandra, D.S. Pandey, J. Inorg. Biochem. 99 (2005) 458–466.
- [12] N. Saglam, A. Colak, S. Dulaer, S. Guner, S. Karabocek, A.O. Belduz, Biometals 15 (2002) 357–365.
- [13] V. Uma, M. Kanthimathi, T. Weyhermuller, B.U. Nair, J. Inorg. Biochem. 99 (2005) 2299–2307.
- [14] Z.D. Xu, H. Liu, S.L. Xiao, M. Yang, X.H. Bu, J. Inorg. Biochem. 90 (2002) 79–84.
- [15] C. Orvig, M.J. Abrams, Chem. Rev. 99 (1999) 2201–2203.
- [16] N. Udilova, V.A. Kozlov, W. Bieberschulte, K. Frei, K. Ehrenberger, H. Nobl, Biochem. Pharmacol. 65 (2003) 59–65.
- [17] H.F. Ji, H.Y. Zhang, Chem. Res. Toxicol. 17 (2004) 471–475.
- [18] S. Adsule, V. Barve, Di Chen, F. Ahmed, Q.P. Dou, S. Padhye, F.H. Sarkar, J. Med. Chem. 49 (2006) 7242–7246.
- [19] P. Nordell, P. Lincoln, J. Am. Chem. Soc. 127 (2005) 9670–9671.
- [20] P. Barraja, P. Diana, A. Montalbano, G. Dattolo, G. Cirrincione, G. Viola, D. Vedaldi, F.D. Acqua, Bioorg. Med. Chem. 14 (2006) 8712–8728.
- [21] A.V. Oeveren, M. Motamedi, E. Martinborough, S. Zhao, Y.S. Xing, S. West, W. Chang, A. Kallem, K.B. Marshchke, F.J. Lopez, N. Andres, L. Zhi, Bioorg. Med. Chem. 17 (2007) 1527–1531.
- [22] J.T. Kuethe, A. Wong, C.X. Qu, J. Smithrovich, I.W. Davies, D.L. Hughes, J. Org. Chem. 70 (2005) 2555–2567.
- [23] N. Amit, M. Alpeshkumar, C. Evans, J. Rahul, Bioorg. Med. Chem. 14 (2006) 7302–7310.
- [24] J. DeRuiter, A.N. Brubaker, W.L. Whitmer, J.L. Stein, J. Med. Chem. 29 (1986) 2024–2028.
- [25] P. Hewawasam, W. Fan, J. Knipe, L.S. Moon, G.C. Boissard, K.V. Gribkoff, E.J. Starett, Bioorg. Med. Chem. Lett. 12 (2002) 1779–1783.
- [26] J. Rousell, E.B. Haddad, J.C. Mak, B.L. Webb, M.A. Giembycz, P.J. Barnes, Mol. Pharmacol. 49 (1996) 629–635.
- [27] I.V. Ukrainets, V.O. Gorokhova, A.P. Benzuglyi, V.L. Sidorenko, Farm. Zh. 1 (2000) 75–80.
- [28] S.Y. Yu, S.X. Wang, Q.H. Luo, L.F. Wang, R.P. Zhou, G. Xing, Polyhedron 12 (1993) 1093–1096.
- [29] S. Padhy, G.B. Kauffman, Coord. Chem. Rev. 63 (1985) 127–160.
- [30] J.G. Wu, R.W. Deng, Z.N. Chen, Trans. Met. Chem. 18 (1993) 23–26.
- [31] S. Chandra, K.K. Sharma, Trans. Met. Chem. 9 (1984) 1–3.
- [32] Z.Y. Yang, B.D. Wang, Y.H. Li, J. Met. Org. Chem. 691 (2006) 4159–4166.
- [33] A.F. Tanius, D.Y. Ding, D.A. Patrick, C. Bailly, R.R. Tidwell, W.D. Wilson, Biochemistry 39 (2002) 12091–12101.
- [34] C.Y. Zhong, J. Zhao, Y.B. Wu, C.X. Yin, P. Yang, J. Inorg. Biochem. 101 (2007) 10–18.
- [35] M.A. Pyle, P.J. Rehmann, R. Meshoyrer, J.N. Kumar, J.N. Turro, K.J. Barton, J. Am. Chem. Soc. 111 (1989) 3053–3063.
- [36] T.R. Li, Z.Y. Yang, B.D. Wang, D.D. Qin, Eur. J. Med. Chem. 43 (2008) 1688–1695.
- [37] A. Alonso, M.J. Almendral, Y. Curto, J.J. Criado, E. Rodriguez, J.L. Manzano, Anal. Biochem. 355 (2006) 157–164.
- [38] J.D. Uram, M. Mayer, Biosens. Bioelectron. 22 (2007) 1556–1560.
- [39] F. Zhang, Y.X. Du, B.F. Ye, P. Li, J. Photochem. Photobiol. B. Biol. 86 (2007) 246–251.
- [40] F.J. Meyer-Almes, D. Porschke, Biochemistry 32 (1993) 4246–4253.
- [41] R.F. Pasternack, M. Caccam, B. Keogh, T.A. Stephenson, A.P. Williams, E.J. Gibbs, J. Am. Chem. Soc. 113 (1991) 6835–6840.
- [42] S. Satyanarayana, J.C. Dabroviak, J.B. Chaires, Biochemistry 31 (1992) 9319–9342.
- [43] D. Lawrence, V.G. Vaidyanathan, B.U. Nair, J. Inorg. Biochem. 100 (2006) 1244–1251.
- [44] N. Yilmaz, H. Dulger, N. Kiyamaz, C. Yilmaz, B.O. Gudu, I. Demir, Brain Res. 1164 (2007) 132–135.
- [45] R. Amorati, F. Ferroni, G.F. Pedulli, L. Valgimigli, J. Org. Chem. 68 (2003) 9654–9658.
- [46] M.K. Singh, A. Chandra, B. Singh, R.M. Singh, Tetrahedron Lett. 48 (2007) 5987–5990.
- [47] G.M. Sheldrick, SHELXTL, Version 6.12, Bruker AXS Inc., Madison, Wisconsin, USA, 2001.
- [48] S.D. Sharma, H.K. Rajor, S. Chopra, R.K. Sharma, Biometals 18 (2005) 143–154.
- [49] T. Ak, İ. Gülçin, Chem. Bio. Interact. 174 (2008) 27–37.
- [50] İ. Gülçin, Chem. Bio. Interact. 179 (2009) 71–80.
- [51] İ. Gülçin, Life Sci. 78 (2006) 803–811.